UC Santa Barbara

UC Santa Barbara Previously Published Works

Title

Designing Protein-Based Probes for Sensing Biological Analytes with Magnetic Resonance Imaging.

Permalink

https://escholarship.org/uc/item/8x51j01k

Journal

Analysis & Sensing, 2(5)

Authors

Yun, Jason
Baldini, Michelle
Chowdhury, Rochishnu
et al.

Publication Date

2022-09-01

DOI

10.1002/anse.202200019

Peer reviewed

eScholarship.org Powered by the California Digital Library
University of California

Author Manuscript

Author Manuscript

Author Manuscript

Author Manuscript

HHS Public Access

Author manuscript

Anal Sens. Author manuscript; available in PMC 2023 July 05.

Published in final edited form as:

Anal Sens. 2022 September ; 2(5): . doi:10.1002/anse.202200019.

Designing Protein-Based Probes for Sensing Biological Analytes with Magnetic Resonance Imaging

Jason Yun[2], **Michelle Baldini**[1], **Rochishnu Chowdhury**[6], **Arnab Mukherjee**[1,2,3,4,5,*]

[1]Department of Chemical Engineering, University of California, Santa Barbara, CA 93106, USA

[2]Department of Chemistry, University of California, Santa Barbara, CA 93106, USA

[3]Biomolecular Science and Engineering, University of California, Santa Barbara, CA 93106, USA

[4]Neuroscience Research Institute, University of California, Santa Barbara, CA 93106, USA

[5]Center for BioEngineering, University of California, Santa Barbara, CA 93106, USA

[6]Mechanical Engineering, University of California, Santa Barbara, CA 93106, USA

Abstract

Genetically encoded sensors provide unique advantages for monitoring biological analytes with molecular and cellular-level specificity. While sensors derived from fluorescent proteins represent staple tools in biological imaging, these probes are limited to optically accessible preparations owing to physical curbs on light penetration. In contrast to optical methods, magnetic resonance imaging (MRI) may be used to noninvasively look inside intact organisms at any arbitrary depth and over large fields of view. These capabilities have spurred the development of innovative methods to connect MRI readouts with biological targets using protein-based probes that are in principle genetically encodable. Here, we highlight the state-of-the-art in MRI-based biomolecular sensors, focusing on their physical mechanisms, quantitative characteristics, and biological applications. We also describe how innovations in reporter gene technology are creating new opportunities to engineer MRI sensors that are sensitive to dilute biological targets.

Introduction

A key frontier of sensor engineering relates to the development of biomolecular probes capable of non-destructively detecting analytes with various imaging modalities. The ability to express such sensors by genetic encoding allows biological processes like cell signaling, neural activity, and enzyme action to be monitored at the molecular level in a wide range of living systems, from cultured cells to intact organisms. Genetic targeting also gives experimental access to well-defined cell types, for example dopaminergic neurons, as well as subcellular locations, thereby achieving a level of specificity that is difficult to match with synthetic labels. Genetically encoded sensors based on fluorescent proteins

*Correspondence should be addressed to AM: arnabm@ucsb.edu, Phone: (805) 893-5137 Rm 3349, Engineering II, Santa Barbara, CA 93106-5080.

CONFLICT OF INTEREST

The authors do not have any conflict of interests to declare.

Author Manuscript Author Manuscript Author Manuscript Author Manuscript

have driven major breakthroughs in virtually all areas of biology, from neural signaling to immune function. However, fluorescent proteins can only be applied in optically accessible preparations due to the limited penetration of light in scattering tissue. Noninvasive technologies are therefore needed to track biological processes at any arbitrary depth inside intact living organisms. In this regard, magnetic resonance imaging (MRI) offers unfettered access to deep tissues, achieving a fairly high spatial resolution (100–400 μm), wide-field coverage, and seconds-scale framerate, while avoiding the use of ionizing radiation. Motivated by these unique advantages, various mechanisms[1–3] have been used to connect MRI contrast with protein-based molecular reporters. Examples of MRI-detectable reporter proteins include iron storage proteins[4–8]; transporters that cause paramagnetic ions like iron, manganese, and gadolinium to accumulate inside cells[9–15]; enzymes that hydrolyze sugars to alter exposure of paramagnetic ions to bulk water[16]; channels that increase the rate of water exchange across the cell membrane[17,18]; vasoactive molecules capable of dilating blood vessels[19,20]; and proteins (or polypeptides) that generate contrast on the basis of chemical exchange between frequency-shifted proton spins and bulk water[21–23]. While these reporters are well-suited for imaging gene expression or tracking the presence and viability of genetically labeled cells *in vivo*[24–26], dynamic sensing of molecular targets requires additional mechanisms to connect biological activity with changes in MRI signals generated by the reporter protein. In this review, we give an overview of the main classes of MRI-based biomolecular sensors, including probes for sensing monoamine neurotransmitters, calcium signals, and enzyme activity. We describe the physical and biochemical basis of various sensing mechanisms, focusing on quantitative aspects of sensor performance, and alongside highlight the key challenges associated with translating these tools to realistic biological applications *in vivo*.

Protein-based MRI sensors for imaging monoamine neurotransmitters

When MRI parameters are chosen to preferentially detect signals arising from the spin-lattice relaxation of water protons (*viz.*, T_1 weighted MRI), image intensity is brightened in the presence of paramagnetic metals harboring one or more water molecules in their coordination sphere. Displacement of water resets the intensity to baseline levels, thereby providing a mechanism (known as q-modulation) to design bio-responsive contrast agents. The first protein reporter to implement q-modulation was beta-galactosidase, which generated T_1 contrast based on enzymatic hydrolysis of a pendant sugar group, thereby restricting water access to a chelated gadolinium ion[16]. This paradigm was later applied to create the first genetically encodable MRI sensor by directed evolution of a heme-binding protein domain (known as BM3h) derived from cytochrome P450[27]. In the absence of the cytochrome's natural substrate (arachidonic acid), water molecules interact directly with the heme-bound iron, leading to faster T_1 relaxation and image brightening (Fig. 1A). Binding of arachidonic acid blocks water access, diminishing T_1 relaxivity (defined as the change in T_1 relaxation rate produced by unit concentration of the sensor) by ~ 3-fold (Fig. 1A). Through iterative rounds of protein engineering by directed evolution, the ligand specificity of BM3h was shifted ~ 84-fold from arachidonic acid (K_d = 750 μM) to the monoamine neurotransmitter, dopamine (K_d = 9 μM), a prime target for molecular MRI due to its role in learning, motor function, and reward processing. Further optimization by

Author Manuscript Author Manuscript Author Manuscript Author Manuscript

structure-guided mutagenesis increased dopamine affinity to ~ 1 μM, yielding a final sensor with ~ 8-fold change in T_1 relaxivity in response to saturating levels of dopamine (Table 1)[28]. By infusing biochemically purified preparations of the engineered sensor (pre-loaded with iron) directly into the rat brain, it was possible to quantitatively map dopamine release and removal kinetics in response to electrical deep brain stimulation (Fig. 1B)[29]. Although these sensors generated modest changes in the MRI signal (on the order of 1 %, Table 1), the approach was able to access dopamine topography across much larger brain volumes (tens of μL) compared to traditional point-measurement techniques like microdialysis, amperometry, and fiber photometry. The heme domain in BM3h further served as a starting point to construct serotonin sensors by structure-guided engineering to increase its binding affinity towards serotonin (K_d = 0.7 μM), with a concomitant reduction in dopamine binding (K_d = 198 μM)[28]. Beyond proof-of-concept, these tools have also revealed new insights on neurochemical signaling in the brain. For example, injection of the dopamine sensor in the striatum, a brain region central to dopamine-dependent reward function, showed that striatal dopamine release is dissociated from local changes in neural activity but correlated with activity in more distal locations like the motor cortex[30]. These findings suggest previously unknown large-scale relationships between neurotransmitter release, clearance, and broader brain activity, which would have been impossible to explore without combining the wide-field capabilities of MRI with the molecular specificity of the BM3h sensor. Likewise, co-infusion of the serotonin sensor with supra-physiological concentrations of serotonin in the rat brain allowed the dynamics of serotonin uptake as well as its inhibition by serotonin reuptake blockers, to be characterized in quantitative voxel-level detail (Fig. 1C)[31]. The same studies also found evidence implicating dopamine transporters in the clearance of extracellular serotonin from the striatum[31]. Notwithstanding these powerful capabilities, the BM3h sensor class also underscores the several general challenges in engineering and applying MRI-based sensors, in particular, their limited sensitivity and dependence on metal precursors. Furthermore, while the BM3h sensors are in principle genetically encodable, it is unlikely that gene expression alone will be able to supply the high protein concentrations (typically 500 μM) required to obtain detectable signal changes in the brain, possibly limiting the main utility of these sensors as injectable probes to be used in conjunction with wide-field brain delivery techniques.

Protein-based MRI sensors for calcium signaling

One of the most widely used techniques for imaging neural activity at the brain-wide scale relies on blood-oxygen level-dependent (BOLD) MRI. Here, T_2 (or T_2*) weighted imaging conditions are employed to detect changes in MRI signal intensity arising from the dephasing of water protons caused by local hemodynamic effects, for example variations in cerebral blood volume, blood flow, and deoxyhemoglobin levels, accompanying neural activity[32,33]. Given that the BOLD signal only indirectly mirrors neural activity, there is tremendous interest in developing noninvasive probes for imaging calcium, an integral molecular signature of electrical activity in all excitable cells. MRI-based calcium sensing has been mostly demonstrated with synthetic labels[34], which are difficult to deliver intracellularly and cannot be targeted to genetically defined cell-types and neural projections. As a first step towards addressing these limitations, a genetically encodable

Author Manuscript Author Manuscript Author Manuscript Author Manuscript

calcium sensor was recently derived from calprotectin, a dual Mn^{2+} and calcium-binding metalloprotein; and applied to monitor calcium changes in Mn^{2+} supplemented cell cultures treated with a calcium ionophore[35]. The contrast mechanism is driven by a dramatic calcium-dependent increase (~ 35-fold) in calprotectin's affinity towards Mn^{2+} ions, causing free Mn^{2+} to become protein-bound and thus unable to shorten the relaxation time of water spins (Fig. 2A).This response is calcium-specific and generates ~ 15 % increase in T_1 relaxation time *in vitro* (Fig. 2B). However, calcium concentrations exceeding the neurobiologically relevant dynamic range (~100 nM to 1 μM) are needed to produce reliable contrast changes. Further improvements in calcium sensitivity, signal amplitude, and intracellular expression will therefore be required to expand calprotectins for monitoring realistic calcium fluctuations in neurons and *in vivo*.

An ingenious approach for calcium sensing was recently developed by exploiting vasoactive biomolecules capable of dilating nearby blood vessels (Fig. 2C). Because vasodilation increases blood flow in the brain, such probes are capable of generating hemodynamic signals similar to BOLD but linked specifically to the vasoactive reporter. This approach was adapted for calcium imaging by engineering neural cells to express neuronal nitric oxide synthase (nNOS), an enzyme activated by calcium-binding to release nitric oxide, a potent vasodilator[36]. To minimize interference from endogenous BOLD signals arising due to neural activity, the catalytic domain of nNOS was swapped with corresponding residues from another nitric oxide-forming enzyme known as inducible NOS (iNOS). Unlike nNOS, iNOS can be selectively inhibited by a small molecule drug without any effect on the BOLD response. The resulting chimeric construct, known as "nitric oxide synthases for targeted image contrast" (NOSTIC), permits BOLD signals to be erased simply by subtracting MRI scans acquired before and after drug infusion. Signal changes (T_2 weighted) in the range of 6 % were obtained in NOSTIC-expressing tumor xenografts infused with a calcium-ionophore to stimulate calcium entry. In conjunction with a retrograde-tracing virus, NOSTICs were applied to successfully map brain regions supplying pre-synaptic inputs to the striatum during electrical deep brain stimulation (Fig. 2D). Furthermore, the amplitude of NOSTIC readouts revealed quantitative differences from (non-specific) fMRI analyses as well as functional connectivity estimates based on cross-correlations between resting state fMRI time traces in the striatum and other brain regions. This work provides (to our knowledge) the very first example of large-scale mapping of brain activity with MRI-based genetic technology, while also highlighting the difficulties of predicting neural information flow using traditional technologies like fMRI that do not reflect molecular signals and cannot be made specific to cell-types or projection fibers.

Biomolecular reporters of protein kinase activity

Kinases comprise a large and functionally diverse family of enzymes with biological roles ranging from receptor-mediated signal transduction to energy storage. Many protein kinases serve as prime targets of small molecule drugs for treating inflammation, cancer, viral infections, and central nervous system disorders. The development of *in vivo* assays for kinase activity is therefore an important goal both for disease research and drug development. Interestingly, kinases, specifically creatine and arginine kinase, represent the very first examples of NMR-detectable reporter genes to be expressed in live animals and

Author Manuscript Author Manuscript Author Manuscript Author Manuscript

monitored noninvasively (albeit without imaging) with ^{31}P spectroscopy[37,38]. The first MRI-based kinase sensor was introduced about two decades later to sense protein kinase A (PKA) activity on the basis of phosphorylation-induced aggregation of the iron storage protein, ferritin[39]. This approach involved two ferritin-based assemblies – one where ferritin was genetically fused to a PKA substrate known as kinase inducible domain (KID); and the other with ferritin fused to a protein domain called KIX that binds phosphorylated KID. Incubation of KID- and KIX-functionalized ferritins with PKA caused the crystals to cluster, generating ~ 83% increase in T_2 relaxivity, attributed to more effective dephasing of water spins due to the larger size of the cluster (Figs. 3A–B, Table 1). Effective contrast generation however required *in vitro* iron loading as well as careful control over the ratio of KID to KIX-containing ferritin as well as the fraction of KID (or KIX) present in each ferritin assembly. Consequently, translating this approach to a fully genetically encoded sensing format in cells (and eventually *in vivo*) has proven challenging. To overcome the dependence on metal precursors, a metal-free sensing paradigm was developed on the basis of chemical exchange saturation transfer (CEST); and applied to monitor PKA activity *in vitro*. The CEST mechanism leverages natural or engineered peptides containing a large number of chemically labile protons, which resonate at frequencies shifted from bulk water. Instead of directly detecting these shifted spins with localized spectroscopy, CEST amplifies sensitivity by first saturating the peptide protons with frequency-selective excitation and subsequently measuring the decrease in (proton-weighted) signal intensity of bulk water caused by the saturated protons exchanging with water protons (Fig. 3C). Given that this exchange process is a key determinant of contrast, CEST-based probes can in principle be designed to sense any biological analyte that alters proton exchange properties (Fig. 3C). Accordingly, a PKA-sensing CEST reporter was developed by fusing eight tandem repeats of the PKA-recognition sequence, Leu-Arg-Arg-Ala-Ser-Leu-Gly[40]. The labile guanidyl and amide protons in arginine generated initial CEST contrast in the range of 2–8 %, 1.8 and 3.6 ppm away from water resonance. Upon serine phosphorylation by PKA, the CEST effect at both frequencies diminished by ~ 50 %, attributed to slowing down of proton exchange due to the presence of the charged phosphate group (Fig. 3D, Table 1). A conceptually analogous sensor was later developed based on a naturally occurring arginine-rich protein, human protamine sulfate, which generated a larger initial CEST contrast (35–40 % at 1.8 ppm, Table 1) and responded similarly to serine phosphorylation, exhibiting a decrease of ~ 30 % in signals[41,42]. While CEST reporter genes have been successfully used to image gene expression in tumor models[23,26], the aforementioned PKA probes have only been demonstrated *in vitro* using bulk purified or synthesized peptides. Key challenges for *in vivo* translation relate to their limited selectivity, for example protamine sulfate was also found to be responsive to pH and nucleotide cofactors[42]; as well as the generally low sensitivity of diamagnetic CEST, typically requiring millimolar probe levels to give detectable contrast. Nevertheless, the ability to produce MRI contrast without any metal dependence, using ~ 50-residue probes, and with multiplexed detection capabilities (based on distinct chemical shifts of exchanging protons) represent unique advantages of the CEST mechanism for developing biomolecular MRI sensors.

Author Manuscript Author Manuscript Author Manuscript Author Manuscript

Biomolecular reporters of protease activity

Proteases perform a wide range of physiological and disease-related functions ranging from tissue remodeling to tumor cell invasion. Like kinases, proteases are also actively pursued as drug targets for a variety of conditions including cancer, liver disease, viral infection, hypertension, and brain injury. Sensitive techniques to assay protease activity *in vivo* are therefore in critical demand both for basic research on disease pathways as well as to facilitate drug development efforts. While several synthetic MRI agents have been developed to sense protease activity, biomolecular (*i.e.*, protein-or peptide-based) reporters are available for two proteases, cathepsin B [43] and fibroblast associated protein (FAP)[44], both of which are highly expressed in tumors and tumor-associated stromal tissue. The cathepsin reporter was designed on the basis of poly-L-glutamate (PLG), which can be cleaved by protease action to release smaller glutamate-containing peptides and individual glutamate moieties[43]. Cathepsin activity therefore increases the availability of free amine groups harboring exchangeable protons, thus generating CEST contrast. While systemic injection of PLG allowed cathepsin activity to be monitored in rat brain tumors (Fig. 4A, Table 1), the sensitivity and precision of this technique were limited, millimolar concentrations of the PLG probe generating ~19 % CEST contrast with modest statistical fidelity (*p-value* in the 0.048 range). In contrast to PLG, detection of FAP[44] was accomplished with much greater sensitivity on the basis of probe-induced vasodilation, similar to the mechanism adopted for calcium sensing with NOSTICs. Here, the probe comprises a calcitonin gene related peptide (CGRP), a 37-residue molecule that binds to a heterodimeric receptor (known as CLR/RAMP) in vascular smooth muscle cells causing dilation of blood vessels, thereby producing MRI contrast[19]. To make CGRP responsive to protease activity, its vasoactive effects were first masked by appending biotinylated FAP-cleavable peptides at the N-terminus. Incubation with FAP removes the blocking group, thereby freeing CGRP to cause vasodilation. Intracranial infusion of the FAP probe, either directly around a tumor xenograft or into the cerebrospinal fluid (for widefield spread) produced mean signal changes in the range of 5–13 %, and further allowed FAP kinetic constants to be computed over the tumor region by solving voxel-level dynamic mass balance equations (Fig. 4B). Given the potent vasodilatory effects of CGRP, infusion of sub-micromolar levels of the probe (~ 100 nM) was found to be sufficient to sense nanomolar-scale FAP concentrations, making this approach the most sensitive MRI-based biomolecular sensing technique reported to date.

Summary and outlook

Genetically encoded sensors afford unique advantages for visualizing biological processes, including (1) access to gene delivery vectors such as neurotropic, axon-tracing, and BBB-crossing viral serotypes, enabling specialized *in vivo* applications in small and large vertebrate species (2) ability to probe specific cell-types with genetic targeting (3) ability to program user-defined temporal profiles, for example by time-locking sensor expression to specific tasks or stimuli (4) compatibility with transgenic animals such as Cre driver lines. The general significance of these capabilities for both basic and applied research is amply borne out by the many scientific breakthroughs enabled by genetically encoded fluorescent indicators, although these tools are limited to optically accessible preparations. MRI offers

Author Manuscript Author Manuscript Author Manuscript Author Manuscript

a diversity of mechanisms to connect analytes with genetically encoded readouts; but a key challenge lies in detecting targets under realistic *in vivo* conditions where biological analytes often span sub- to mid-μM dynamic range. Ultrasensitive detection with MRI has traditionally relied on (non-genetic) magnetic nanoparticles that can be applied at nanomolar particle concentrations. While ferritin can be assembled inside cells with genetic techniques, the ensuing relaxivity is much smaller than similarly-sized synthetic nanoparticles, which limits the sensitivity of the clustering mechanism for ferritin-based biosensing[45]. That said, the recent advent of several engineered iron-nucleating proteins with higher per-particle magnetic moments[19,46–49] compared to ferritin provides a fresh set of biomolecular templates that could be used to sense dilute analytes based on nanoscale assembly and aggregation. The general feasibility of this approach has already been established by imaging streptavidin in yeast cells engineered to express a hypermagnetic variant of ferritin fused with streptavidin-binding peptides[50]. Alongside these developments in metalloprotein-based reporters, a stream of advances in new metal-free MRI mechanisms including hemodynamic imaging, diffusion-weighted MRI, and hyperpolarized xenon imaging could open further avenues for amplifying sensitivity. For instance, vasoactive probes boost detection limits by exploiting the innate potency of vasodilatory peptides, which tend to operate at effective concentrations in the nanomolar range (*e.g.*, EC_{50} of CGRP ~ 10 nM)[19]. Diffusion imaging taps into the fast and highly selective transport of water molecules through channels like aquaporins, resulting in an increase in transmembrane water exchange rate in cells, making them detectable with MRI techniques weighted towards spin diffusion[17,18]. Hyperpolarization of ^{129}Xe amplifies their MRI signals by 4–5 orders of magnitude over thermally polarized spins, dramatically improving sensitivity. By using specialized femtoliter-sized protein compartments (called gas vesicles) to contain the hyperpolarized xenon molecules, it becomes possible to detect gas vesicles at concentrations even lower than the nanomolar doses of radioactive tracers typically used in nuclear imaging[51]. Unlike vasodilatory probes, gas vesicles and water channels have not (yet) been applied for MRI-based biosensing. However, efforts are underway to connect their unique biophysical properties with biological activity using protein engineering, for example, gas vesicles have already been engineered to probe protease activity with ultrasound[52]. Despite these advances, detection of particularly dilute targets with MRI could be considerably challenging, especially if these targets only fleetingly reach their peak amplitudes or are sparsely distributed among cells, for example voltage changes and nitric oxide signals. In these cases, it may be more practical to design MRI-based molecular integrators that convert transient signal changes to a more lasting change in the relaxivity or expression of an MRI reporter gene. Similar methods are already used in optical imaging to record neural activity over experimentally defined epochs by integration of transient calcium rises[53]. In conclusion, we anticipate that innovations in sensor engineering will go hand-in-hand with advances in MRI technology, ultimately allowing a much broader repertoire of biological analytes to be tracked in vertebrate species of all sizes, with a combination of seconds-scale kinetics, widefield coverage, and spatial resolution potentially reaching the sub-100 μm range (theoretical limit is around 10 μm[54]).

Author Manuscript Author Manuscript Author Manuscript Author Manuscript

ACKNOWLEDGEMENTS

We thank all current and former members of the Mukherjee lab as well as our collaborators for helpful discussions. We especially thank Prof. Mikhail Shapiro (Caltech) for many insightful discussions on the topic of this review. Work related to this review has been supported by the California NanoSystems Institute, a NARSAD Young Investigator Award from the Brain and Behavior Research Foundation (to AM), National Institutes of Health R35 Maximizing Investigators' Research Award (to AM), and support from the Army's Institute of Collaborative Biotechnologies (to AM). Dr. Jason Yun acknowledges support from the 2021 Chair's Fellowship, Department of Chemistry, UCSB. Michelle Baldini is a recipient of the Regent's Fellowship (UCSB) as well as a Graduate Research Fellowship from the National Science Foundation.

LIST OF ABBREVIATIONS USED IN THE MANUSCRIPT

MRI	magnetic resonance imaging
CEST	chemical exchange saturation transfer
CGRP	calcitonin gene related peptide
nNOS	neuronal nitric oxide synthase
FAP	fibroblast associated protein

REFERENCES

[1]. Gilad AA, Winnard PT, van Zijl PCM, Bulte JWM, NMR Biomed 2007, 20, 275–290. [PubMed: 17451181]

[2]. Mukherjee A, Davis HC, Ramesh P, Lu GJ, Shapiro MG, Progress in Nuclear Magnetic Resonance Spectroscopy 2017, 102–103, 32–42.

[3]. Gilad AA, Shapiro MG, Molecular Imaging and Biology 2017, 19, 373–378. [PubMed: 28213833]

[4]. Cohen B, Ziv K, Plaks V, Israely T, Kalchenko V, Harmelin A, Benjamin LE, Neeman M, Nat. Med 2007, 13, 498–503. [PubMed: 17351627]

[5]. Iordanova B, Robison CS, Ahrens ET, Journal of Biological Inorganic Chemistry 2010, 15, 957–965. [PubMed: 20401622]

[6]. Cohen B, Dafni H, Meir G, Harmelin A, Neeman M, Neoplasia 2005, 7, 109–117. [PubMed: 15802016]

[7]. Genove G, DeMarco U, Xu H, Goins WF, Ahrens ET, Nature Medicine 2005, 11, 450–454.

[8]. Zurkiya O, Chan AWS, Hu X, Magnetic Resonance in Medicine 2008, 59, 1225–1231. [PubMed: 18506784]

[9]. Patrick PS, Hammersley J, Loizou L, Kettunen MI, Rodrigues TB, Hu DE, Tee SS, Hesketh R, Lyons SK, Soloviev D, Lewis DY, Aime S, Fulton SM, Brindle KM, Proc. Natl Acad. Sci. USA 2014, 111, 415–420. [PubMed: 24347640]

[10]. Patrick PS, Rodrigues TB, Kettunen MI, Lyons SK, Neves AA, Brindle KM, Magn. Reson. Med 2016, 75, 1697–1707. [PubMed: 25981669]

[11]. Deans AE, Wadghiri YZ, Bernas LM, Yu X, Rutt BK, Turnbull DH, Magn. Reson. Med 2006, 56, 51–59. [PubMed: 16724301]

[12]. Bartelle BB, Szulc KU, Suero-Abreu GA, Rodriguez JJ, Turnbull DH, Magnetic Resonance in Medicine 2013, 70, 842–850. [PubMed: 23065715]

[13]. Bartelle BB, Mana MD, Suero-Abreu GA, Rodriguez JJ, Turnbull DH, Magn. Reson. Med 2015, 74, 1750–1757. [PubMed: 25522343]

[14]. Högemann-Savellano D, Bost E, Blondet C, Sato F, Abe T, Josephson L, Weissleder R, Gaudet J, Sgroi D, Peters PJ, Basilion JP, Neoplasia 2003, 5, 495–506. [PubMed: 14965443]

[15]. Weissleder R, Simonova M, Bogdanova A, Bredow S, Enochs WS, Bogdanov A, https://doi.org/10.1148/radiology.204.2.9240530 1997, 204, 425–429.

Author Manuscript Author Manuscript Author Manuscript Author Manuscript

[16]. Louie AY, Hüber MM, Ahrens ET, Rothbächer U, Moats R, Jacobs RE, Fraser SE, Meade TJ, Nat. Biotechnol 2000, 18, 321–325. [PubMed: 10700150]

[17]. Schilling F, Ros S, Hu DE, D'Santos P, McGuire S, Mair R, Wright AJ, Mannion E, Franklin RJM, Neves AA, Brindle KM, Nature Biotechnology 2017, 35, 75–80.

[18]. Mukherjee A, Wu D, Davis HC, Shapiro MG, Nature Communications 2016 7:1 2016, 7, 1–9.

[19]. Desai M, Slusarczyk AL, Chapin A, Barch M, Jasanoff A, Nature Communications 2016 7:1 2016, 7, 1–10.

[20]. Ohlendorf R, Wiśniowska A, Desai M, Barandov A, Slusarczyk AL, Li N, Jasanoff A, Nature Communications 2020 11:1 2020, 11, 1–10.

[21]. Bar-Shir A, Liang Y, Chan KWY, Gilad AA, Bulte JWM, Chemical Communications 2015, 51, 4869–4871. [PubMed: 25697683]

[22]. Gilad AA, McMahon MT, Walczak P, Winnard PT, Raman V, van Laarhoven HWM, Skoglund CM, Bulte JWM, van Zijl PCM, Nature Biotechnology 2007, 25, 217–219.

[23]. Allouche-Arnon H, Khersonsky O, Tirukoti ND, Peleg Y, Dym O, Albeck S, Brandis A, Mehlman T, Avram L, Harris T, Yadav NN, Fleishman SJ, Bar-Shir A, Nature Biotechnology 2022 2022, 1–7.

[24]. Iordanova B, Ahrens ET, Neuroimage 2012, 59, 1004–1012. [PubMed: 21939774]

[25]. Kelly JJ, Saee-Marand M, Nyström NN, Evans MM, Chen Y, Martinez FM, Hamilton AM, Ronald JA, Science Advances 2021, 7, DOI 10.1126/SCIADV.ABC3791/SUPPL_FILE/ABC3791_SM.PDF.

[26]. Minn I, Bar-Shir A, Yarlagadda K, Bulte JWM, Fisher PB, Wang H, Gilad AA, Pomper MG, Magnetic Resonance in Medicine 2015, 74, 544–549. [PubMed: 25919119]

[27]. Shapiro MG, Westmeyer GG, Romero PA, Szablowski JO, Küster B, Shah A, Otey CR, Langer R, Arnold FH, Jasanoff A, Nat. Biotechnol 2010, 28, 264–270. [PubMed: 20190737]

[28]. Brustad EM, Lelyveld VS, Snow CD, Crook N, Jung ST, Martinez FM, Scholl TJ, Jasanoff A, Arnold FH, Journal of Molecular Biology 2012, 422, 245–262. [PubMed: 22659321]

[29]. Lee T, Cai LX, Lelyveld VS, Hai A, Jasanoff A, Science (1979) 2014, 344, 533–535.

[30]. Li N, Jasanoff A, Nature 2020, 580, 239–244. [PubMed: 32269346]

[31]. Hai A, Cai LX, Lee T, Lelyveld VS, Jasanoff A, Neuron 2016, 92, 754–765. [PubMed: 27773583]

[32]. Heeger DJ, Ress D, Nature Reviews Neuroscience 2002 3:2 2002, 3, 142–151.

[33]. Logothetis NK, Nature 2008 453:7197 2008, 453, 869–878.

[34]. Miller ADC, Ozbakir HF, Mukherjee A, Chemical Physics Reviews 2021, 2, 021301. [PubMed: 34085055]

[35]. Ozbakir HF, Miller ADC, Fishman KB, Martins AF, Kippin TE, Mukherjee A, ACS Sensors 2021, 6, 3163–3169. [PubMed: 34420291]

[36]. Ghosh S, Li N, Schwalm M, Bartelle BB, Xie T, Daher JI, Singh UD, Xie K, DiNapoli N, Evans NB, Chung K, Jasanoff A, Nature Neuroscience 2022, 25, 390–398. [PubMed: 35241803]

[37]. Koretsky AP, Brosnan MJ, Chen L, Chen J, van Dyke T, Proc Natl Acad Sci U S A 1990, 87, 3112–3116. [PubMed: 2326269]

[38]. Walter G, Barton ER, Sweeney HL, Proc Natl Acad Sci U S A 2000, 97, 5151–5155. [PubMed: 10805778]

[39]. Shapiro MG, Szablowski JO, Langer R, Jasanoff A, J Am Chem Soc 2009, 131, 2484–2486. [PubMed: 19199639]

[40]. Airan RD, Bar-Shir A, Liu G, Pelled G, McMahon MT, van Zijl PCM, Bulte JWM, Gilad AA, Magnetic Resonance in Medicine 2012, 68, 1919–1923. [PubMed: 23023588]

[41]. Bar-Shir A, Liu G, Chan KWY, Oskolkov N, Song X, Yadav NN, Walczak P, McMahon MT, van Zijl PCM, Bulte JWM, Gilad AA, ACS Chem. Biol 2013, 9, 134–138. [PubMed: 24138139]

[42]. Oskolkov N, Bar-Shir A, Chan KWY, Song X, van Zijl PCM, Bulte JWM, Gilad AA, McMahon MT, ACS Macro Letters 2015, 4, 34–38. [PubMed: 25642384]

[43]. Haris M, Singh A, Mohammed I, Ittyerah R, Nath K, Nanga RPR, Debrosse C, Kogan F, Cai K, Poptani H, Reddy D, Hariharan H, Reddy R, Scientific Reports 2014, 4, DOI 10.1038/srep06081.

Author Manuscript Author Manuscript Author Manuscript Author Manuscript

[44]. Desai M, Sharma J, Slusarczyk AL, Chapin AA, Ohlendorf R, Wisniowska A, Sur M, Jasanoff A, n.d., DOI 10.7554/eLife.

[45]. Bulte JWM, Douglas T, Mann S, Frankel RB, Moskowitz BM, Brooks RA, Baumgarner CD, Vymazal J, P Strub M, Frank JA, Journal of Magnetic Resonance Imaging 1994, 4, 497–505. [PubMed: 7802866]

[46]. Sigmund F, Massner C, Erdmann P, Stelzl A, Rolbieski H, Desai M, Bricault S, Wörner TP, Snijder J, Geerlof A, Fuchs H, de Angelis MH, Heck AJR, Jasanoff A, Ntziachristos V, Plitzko J, Westmeyer GG, Nature Communications 2018, 9, DOI 10.1038/s41467-018-04227-3.

[47]. Ramesh P, Hwang S, Davis HC, Lee Gosselin A, Bharadwaj V, English MA, Sheng J, Iyer V, Shapiro MG, Angewandte Chemie 2018, 130, 12565–12569.

[48]. Liu X, Lopez PA, Giessen TW, Giles M, Way JC, Silver PA, Scientific Reports 2016 6:1 2016, 6, 1–10.

[49]. Radoul M, Lewin L, Cohen B, Oren R, Popov S, Davidov G, Vandsburger MH, Harmelin A, Bitton R, Greneche JM, Neeman M, Zarivach R, Scientific Reports 2016 6:1 2016, 6, 1–9.

[50]. Matsumoto Y, Chen R, Anikeeva P, Jasanoff A, Nat. Commun 2015, 6, 8721. [PubMed: 26522873]

[51]. Shapiro MG, Ramirez RM, Sperling LJ, Sun G, Sun J, Pines A, Schaffer D. v., Bajaj VS, Nat. Chem 2014, 6, 629–634. [PubMed: 24950334]

[52]. Lakshmanan A, Jin Z, Nety SP, Sawyer DP, Lee-Gosselin A, Malounda D, Swift MB, Maresca D, Shapiro MG, Nature Chemical Biology 2020 16:9 2020, 16, 988–996.

[53]. Kim CK, Sanchez MI, Hoerbelt P, Fenno LE, Malenka RC, Deisseroth K, Ting AY, Cell 2020, 183, 2003–2019.e16. [PubMed: 33308478]

[54]. Krug JR, van Schadewijk R, Vergeldt FJ, Webb AG, de Groot HJM, Alia A, van As H, Velders AH, 2020, DOI 10.1016/j.jmr.2020.106770.

Author Manuscript Author Manuscript Author Manuscript Author Manuscript

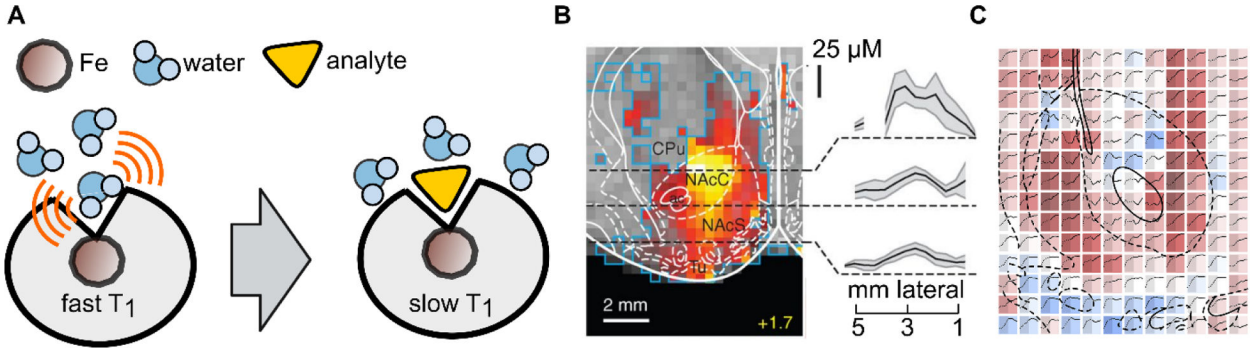

Figure 1. Biomolecular MRI probes for imaging monoamine neurotransmitters.

(A) The sensing mechanism is based on changes in exposure of protein-bound iron ions to water molecules induced by binding to a neurotransmitter analyte, which generates T_1 weighted contrast. (B) Voxel-level mapping of peak dopamine concentrations released in the striatum by electrical deep brain stimulation. (c) Voxel-level mapping of percent change in T_1 weighted signals following striatal infusion of a mixture of serotonin + BM3h sensor *vs.* sensor-only. The time course of signal change post-infusion is shown as an inset in each voxel. Images in (B) and (C) are reproduced with permission from references [29] and [31].

Author Manuscript Author Manuscript Author Manuscript Author Manuscript

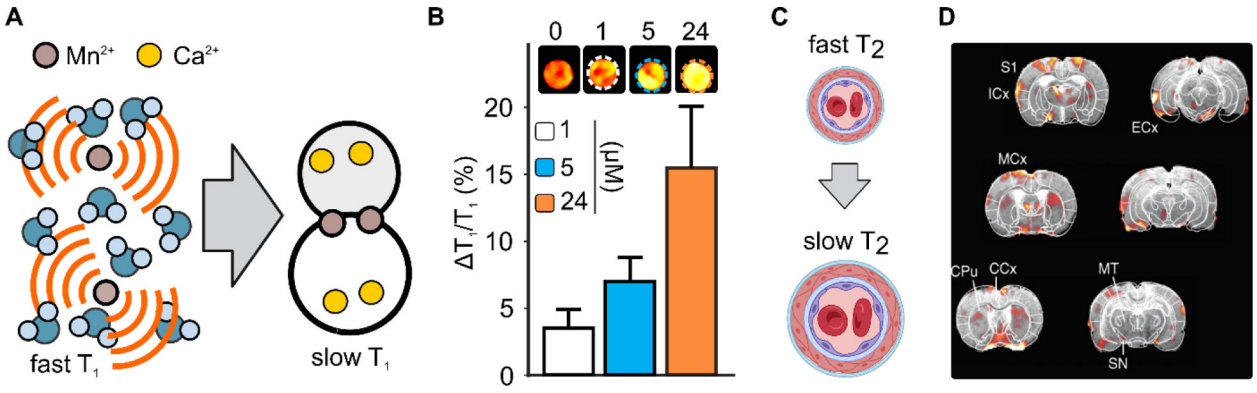

Figure 2.

Genetically encoded MRI-based calcium indicators. (A) Calcium sensing in calprotectin is based on calcium-induced binding of free Mn^{2+} to calprotectin, which reduces the T_1 relaxation rate. (B) Calcium can be detected in the double-digit micromolar range *in vitro* using biochemically purified preparations of calprotectin. (C) Hemogenetic imaging leverages a calcium-activated vasoactive probe to produce nitric oxide, thereby dilating cerebral arterioles in response to calcium rises. (D) Noninvasive detection of calcium signals in brain locations that send neural inputs to the striatum during deep brain stimulation. Images in (A) and (B) are reproduced with permission from reference [35]. Image in (D) is reproduced with permission from reference [36].

Author Manuscript Author Manuscript Author Manuscript Author Manuscript

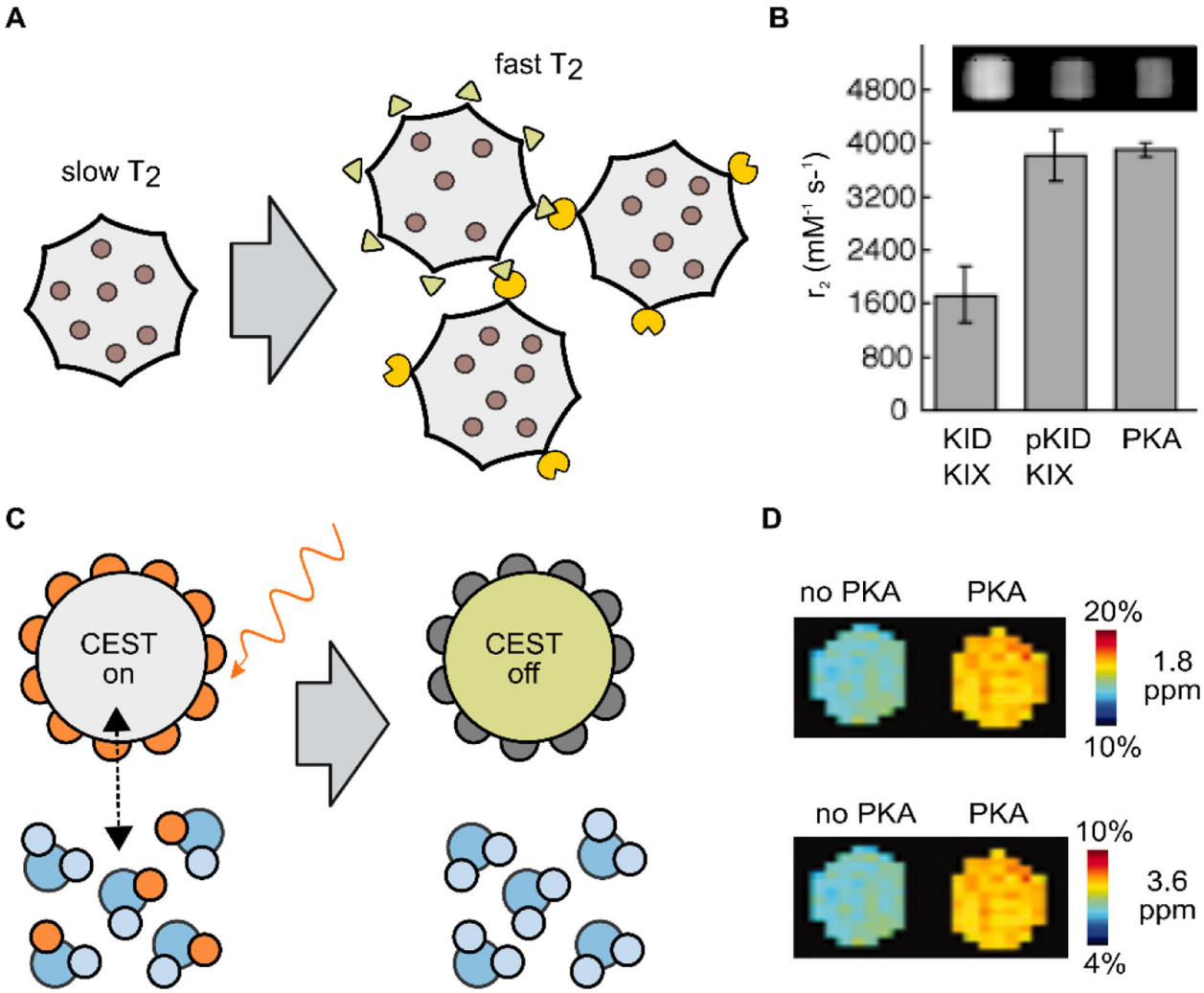

Figure 3. Biomolecular reporters of protein kinase activity.

(A) Protein nanoparticles like ferritin generate contrast on the basis of analyte-induced clustering, which produces changes in their T_2 relaxation rate. (B) Faster T_2 leads to darkening of T_2 weighted images acquired using purified mixtures of KID and KIX-functionalized ferritins incubated with protein kinase A (PKA). (C) CEST probes typically rely on analyte-induced changes in exchange rates of chemically labile protons that can be selectively saturated with a radiofrequency pulse. (D) The CEST-based PKA sensor monitors phosphorylation-induced changes in signal intensity at 1.8 and 3.6 ppm. Images in (B) and (D) are reproduced with permission from references [39] and [40].

Author Manuscript Author Manuscript Author Manuscript Author Manuscript

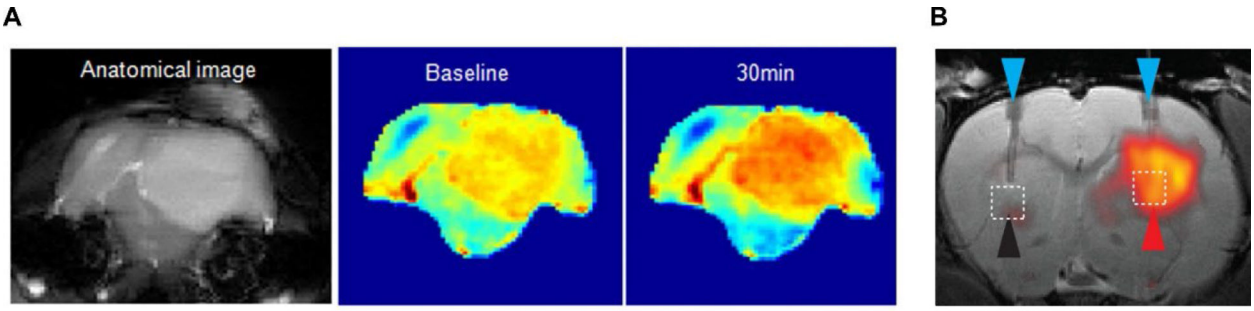

Figure 4. MRI-based biomolecular sensors of protease activity.

(A) Imaging cathepsin activity in a gliosarcoma tumor by intravenous injection of poly-L-glutamate that produces CEST contrast upon protease cleavage. (B) Imaging FAP protease activity in a genetically engineered tumor model, by intracranial infusion of a vasoactive probe that acts on endothelial cell-surface receptors to cause vasodilation following protease cleavage and removal of a masking group. Images in (A) and (B) are reproduced with permission from references [43] and [44] via a Creative Commons Attribution 4.0 International License: https://creativecommons.org/licenses/by/4.0/.

Author Manuscript Author Manuscript Author Manuscript Author Manuscript

Table 1.

Key quantitative aspects of biomolecular MRI sensors

Protein	analyte	on state[a] (*in vitro*)	off state[a] (*in vitro*)	ΔS/S (*in vivo*)	size (kDa)	injected dose
BM3h[27,29]	dopamine	0.10 $mM^{-1}\ s^{-1}$	0.83 $mM^{-1}\ s^{-1}$	1 %	53	[b]5 nmol
BM3h[31]	serotonin	0.19 $mM^{-1}\ s^{-1}$	0.99 $mM^{-1}\ s^{-1}$	9 %	53	[b]3 nmol
NOSTIC[36]	calcium	-	-	2 %	157	
Calprotectin[35]	calcium	0.2 $mM^{-1}\ s^{-1}$	5.2 $mM^{-1}\ s^{-1}$	-	24	-
Ferritin[39]	PKA	2120 $mM^{-1}\ s^{-1}$	3900 $mM^{-1}\ s^{-1}$	-	480	-
$(LRRASLG)_{8x}$[40]	PKA	~8 %	< 4 %	-	6.8	-
Protamine sulfate[42]	kinase	~40 %	~25 %	-	6.9	-
poly-L-glutamate[43]	cathepsin	~22 %	~26 %	19 %	-	[c]160 mg/kg
CGRP[44]	FAP	-	-	5 %	3.7	[d]1 pmol

[a] On and off-state values either represent relaxivity measurements (for T_1 and T_2 probes) or percent signal change (for CEST probes) acquired with bulk-purified or chemically synthesized preparations of the respective sensor in the presence or absence of saturating concentrations of their target analyte;

[b] these probes were delivered by intracranial infusion;

[c] intravenous injection;

[d] intra-CSF infusion. The absolute number of moles infused is estimated based on the reported values of infusion rate *x* duration of injection *x* probe concentration.